REDUCTION FACTORS FOR CREEP STRENGTH AND FATIGUE LIFE OF MODIFIED 9 CR-1 MO STEEL WELDMENTS

Confirmation By Axial or Torsional Tests of Tubular Specimens With Longitudinal or Circumferential Welds*

J.J. Blass
R. L. Battiste
D.G. O'Connor

Oak Ridge National Laboratory
Oak Ridge, Tennessee 37831-8051

ABSTRACT

The provisions of ASME B&PV Code Case N-47 currently include reduction factors for creep strength and fatigue life of weldments. To provide experimental confirmation of such factors for modified 9 Cr-1 Mo steel, tests of tubular specimens were conducted at 538°C (1000°F).

Three creep-rupture specimens with longitudinal welds were tested in tension; and, of three with circumferential welds, two were tested in tension and one in torsion. In each specimen with a circumferential weld, a nonuniform axial distribution of strain was easily visible. The test results were compared to an existing empirical model of creep-rupture life. For the torsion test, the comparison was based on a definition of equivalent normal stress recently adopted in Code Case N-47.

Some 27 fatigue specimens, with longitudinal, circumferential, or no welds, were tested under axial or torsional strain control. In specimens with welds, fatigue cracking initiated at fusion lines. In axial tests cracks grew in the circumferential direction, and in torsional tests cracks grew along fusion lines. The test results were compared to empirical models of fatigue life based on two definitions of equivalent normal strain range.

The results have provided some needed confirmation of the reduction factors for creep strength and fatigue life of modified 9 Cr-1 Mo steel weldments currently under consideration by ASME Code committees.

INTRODUCTION

The provisions of ASME Boiler and Pressure Vessel Code Case N-47 (*Class 1 Components in Elevated Temperature Service*, Section III, Division 1) currently include reduction factors for creep strength and fatigue life of weldments. Corum (1990) discussed the reasons and bases for these factors, and evaluated the results of confirmatory creep-rupture and continuous-cycling fatigue tests of 316 stainless steel weldments. Such factors are currently under consideration by appropriate ASME Code committees for modified 9 Cr-1 Mo steel weldments.

The creep-strength reduction factors were based on the results of creep-rupture tests of small, solid-bar specimens of modified 9 Cr-1 Mo steel and its weldments (Brinkman et al., 1990). The uniform-diameter gage sections of the weldment specimens contained weld, heat affected zone (HAZ), and parent metal. For a given temperature and a given rupture time, the reduction factor is the ratio of average weldment strength to average parent-metal strength.

Some continuous-cycling fatigue tests have been conducted on small, solid-bar specimens taken from weldments of modified 9 Cr-1 Mo steel (Payne, 1986). The results were consistent with the basis for the fatigue-life reduction factor of two currently used in Code Case N-47 for other materials.

To provide additional experimental confirmation of these factors, axial or torsional tests at 538°C (1000°F), of tubular specimens with longitudinal or circumferential welds, were conducted at Oak Ridge National Laboratory (ORNL) as described herein.

TUBULAR TEST SPECIMENS

Tubular specimens of modified 9 Cr-1 Mo steel, each containing a pair of longitudinal welds, a single circumferential weld, or no weld, were fabricated from 51-mm (2.0-in.)-thick plate of heat 30383. The longitudinal axis of each specimen was parallel to the rolling direction of the plate. The fabrication process was as follows.

The plate material was sawed into pieces wide enough for three specimens side by side, and long enough for two fatigue specimens end to end. The plates were normalized by heating to 1038°C (1900°F), holding for 1.5 h, and air cooling. They were tempered by heating to 760°C (1400°F), holding for 1.5 h, and air cooling. Grooves for the longitudinal welds were machined along the longitudinal centerlines of the top and bottom surfaces of the plates, as shown in Fig. 1(a). With the plates preheated to 200°C (392°F), the grooves were filled with modified 9 Cr-1 Mo weld metal using a manual gas-tungsten-arc (GTA) process. The filler wire was from United States Welding Corp., specification DRV 1513, heat 23030, lot 49005.

The plates were sawed into pieces of specimen size, and these were machined into 51-mm (2.0-in.)-diameter bars. Grooves for the circumferential welds were machined in some of the bars without longitudinal welds, as shown in Fig. 1(b). These grooves were filled with weld metal using the same wire and process as the longitudinal welds. The welds were radiographed, and no flaws were detected. The bars, including those without welds, were given a post-weld heat treatment of 1.5 h at 760°C (1400°F), followed by air cooling.
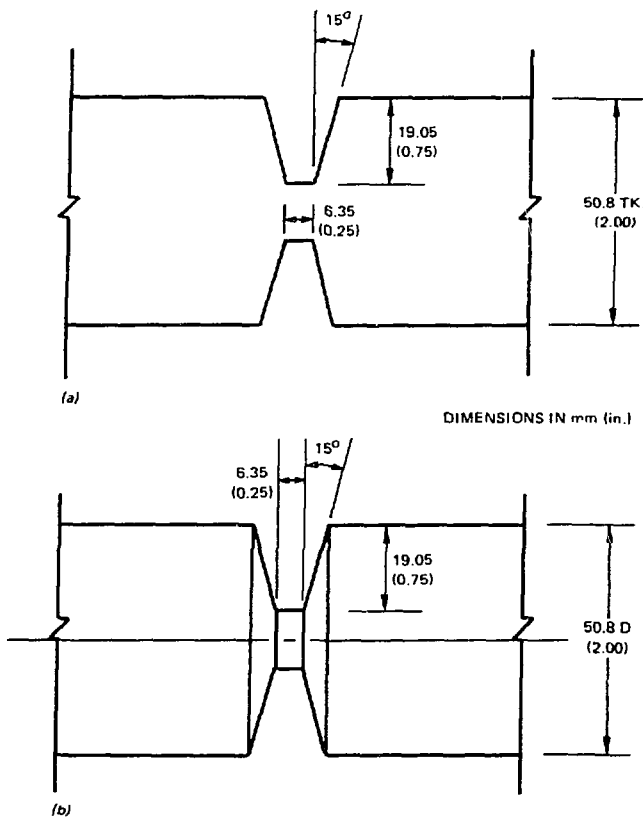
Fig. 1. Weld grooves for tubular specimens. (a) Longitudinal grooves in flat plate. (b) Circumferential groove in round bar.

Fig. 2. Weld locations and specimen details. (a) Method of obtaining tubular specimens with welds. (b) Dimensions of creep-rupture specimen.

The method of obtaining tubular specimens with longitudinal or circumferential welds is illustrated in Fig. 2(a). Six creep-rupture specimens, three with longitudinal and three with circumferential welds, were machined to the final dimensions shown in Fig. 2(b). Fatigue specimens were machined from the remaining bars, including those without welds. The dimensions of the reduced section of the fatigue specimen were identical to those of the creep specimen shown in Fig. 2(b). However, the 44-mm (1.75-in.)-diameter ends of the fatigue specimen were 140 mm (5.5 in.) long, and were not internally threaded because external collet grips were used.

Based on the groove dimensions shown in Fig. 1, each weld was nominally 8.5 mm (0.33 in.) wide at the outer surface of the tubular specimen. Hardness measurements were made at room temperature on the outer surface of the uniform-diameter portions of an untested specimen with a circumferential weld. Within the band of weld metal at mid-length, the measurements corresponded to about 101 on the Rockwell-B scale. As axial distance from the weld increased, there was an approximately linear decrease in hardness, to about 78 Rockwell B slightly beyond each end of the 25.4-mm (1.00-in.) gage length, indicating that the HAZ extended at least that far. The hardness of the base metal at the large-diameter ends of the specimen was about 92 Rockwell B. The variation in hardness is indicative of a variation in inelastic response that can result in a nonuniform axial distribution of strain in the gage length. In effect, the specimen contains a "metallurgical notch" (Corum, 1990).

CREEP-RUPTURE TESTS

To provide experimental confirmation of the creep-strength reduction factors, axial or torsional creep-rupture tests of tubular
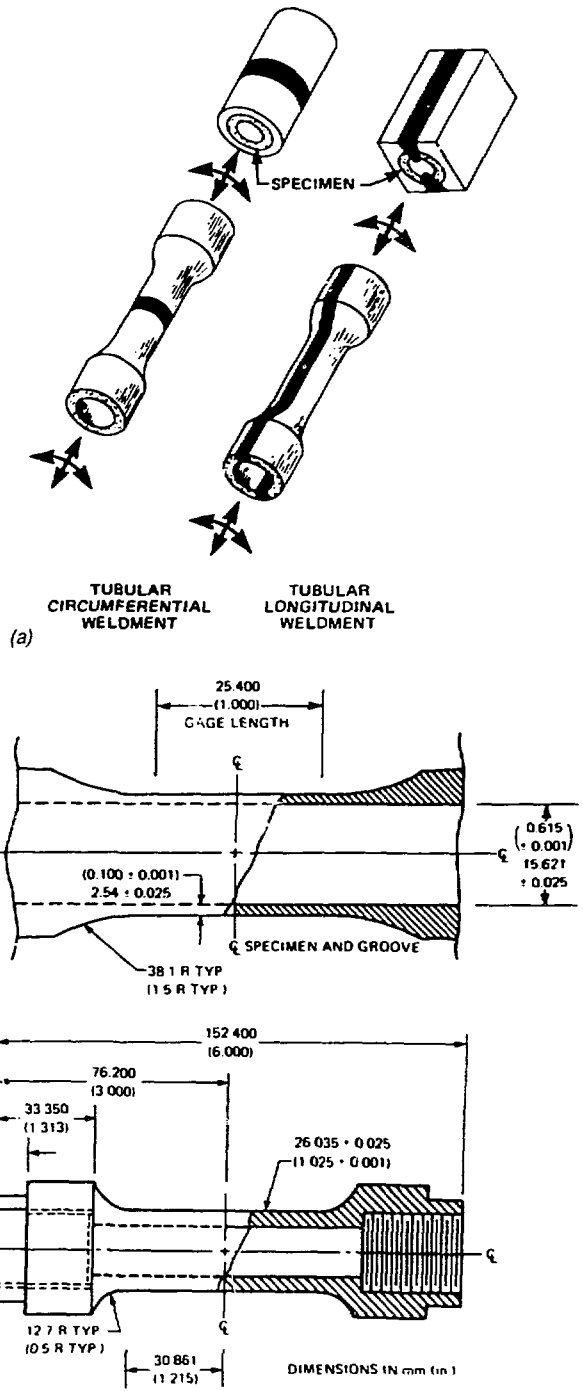
specimens, with longitudinal or circumferential welds, were conducted in air at 538°C (1000°F). As described above, three specimens were fabricated with longitudinal welds, and three with circumferential welds. One of the specimens with a circumferential weld was subjected to torsional loading, and the other five specimens

to axial loading, in axial-torsional creep machines originally developed by K.C. Liu and modified by R.L. Battiste at ORNL.

In each specimen with a circumferential weld, a nonuniform axial distribution of axial or torsional strain was easily visible after the test, with weld metal exhibiting less strain than adjacent HAZ metal. This is attributed to the metallurgical notch.

The test results are plotted in Fig. 3 as equivalent stress versus time to rupture, with different symbols to distinguish between the two weld orientations and a label to identify the torsion test. The definition of equivalent normal stress used for the torsion test was proposed by Huddleston (1985). In its most general form, the definition contains two parameters, designated a and b, for which optimum values may be obtained from the results of multiaxial creep-rupture tests of a given material. Since slightly different optimum values were obtained for similar materials, generic values $a = 1.0$ and $b = 0.24$ were recommended for austenitic steels (Huddleston, 1985). For $a = 1.0$, the definition reduces to the form adopted in 1990 for use in Appendix T of Code Case N-47:

$$\sigma_{eq} = \overline{\sigma} \exp\{b[(J_1 / S_s) - 1]\} \qquad (1a)$$

where

$$\overline{\sigma}^2 = [(\sigma_1 - \sigma_2)^2 + (\sigma_2 - \sigma_3)^2 + (\sigma_3 - \sigma_1)^2]/2 \qquad (1b)$$

$$J_1 = \sigma_1 + \sigma_2 + \sigma_3 \qquad (1c)$$

$$S_s^2 = \sigma_1^2 + \sigma_2^2 + \sigma_3^2 \qquad (1d)$$

and σ_1, σ_2 and σ_3 are principal stresses. For axial-torsional loading of tubular specimens, it further reduces to

$$\sigma_{eq} = \sqrt{\sigma_z^2 + 3\tau_{\theta z}^2} \exp\left\{b\left[\left(\sigma_z / \sqrt{\sigma_z^2 + 2\tau_{\theta z}^2}\right) - 1\right]\right\} \qquad (2)$$

where σ_z is axial stress and $\tau_{\theta z}$ is torsional shear stress. Since the present tests were either purely axial or purely torsional, the equivalent stress becomes

$$\sigma_{eq} = \sigma_z, \text{ for } \tau_{\theta z} = 0, \qquad (3a)$$

or

$$\sigma_{eq} = \sqrt{3}\tau_{\theta z} / \exp(b), \text{ for } \sigma_z = 0. \qquad (3b)$$

The recommended value $b = 0.24$ was adopted in Appendix T for 304 and 316 stainless steels, and the default value $b = 0.0$ was adopted for Alloy 800H and 2 25 Cr-1 Mo steel, pending further evaluation. With $b = 0.0$, Eq. (1) reduces to $\sigma_{eq} = \overline{\sigma}$, the Mises equivalent stress, used in Appendix T until the present. Based largely on an unpublished evaluation of the results of some internal-pressure tests of 2.25 Cr-1 Mo tubes, Huddleston (1990) would have tentatively recommended the generic value $b = 0.16$ for ferritic steels, including modified 9 Cr-1 Mo. This value was used to calculate σ_{eq} for the torsion test identified in Fig. 3. If the values $b = 0.0$ or 0.24 were used, σ_{eq} would be 17% greater or 8% less, respectively. In either case, the torsion test would be less consistent with the axial tests.

In addition to the results for welded tubes, three lines are plotted in Fig. 3, corresponding to specific applications of the creep-rupture model (Brinkman et al., 1990) for modified 9 Cr-1 Mo steel:

$$\log t_r = C_h - 0.231\sigma - 2.385 \log \sigma + 31,080 / T \qquad (4)$$

where logarithms are base 10, t_r is rupture time (h), σ is stress (MPa) and T is absolute temperature (K). The parameter C_h is a constant for a specific lot of material, assuming the same dependence of rupture time on stress and temperature for all lots. The uppermost dotted line in the figure corresponds to $C_h = -23.414$, a value based on only one test at 538°C (1000°F) and one at 593°C (1100°F) of specimens from 51-mm (2.0-in.) plate of heat 30383, the lot of parent material from which the tubular specimens were fabricated. The intermediate solid line corresponds to $C_h = -23.737$ for average parent material, and the lowermost dashed line corresponds to $C_h = -24.257$ for average material from weldments. The lowermost dashed line also corresponds closely to $C_h = -24.272$ for minimum creep-rupture strength of parent metal.

For a given temperature and a given rupture time, the creep-strength reduction factor in Code Case N-47 is the ratio of average weldment strength to average parent-metal strength. For modified 9 Cr-1 Mo steel, the strength values were obtained by numerical solution of Eq. (4) with the appropriate values of C_h (Brinkman et al., 1990). For a temperature of 538°C (1000°F) and rupture times of 10^1, 10^3 and 10^5 h, for example, the ratios are 0.94, 0.93 and 0.90, respectively. The two lower lines in Fig. 3 are perfectly consistent
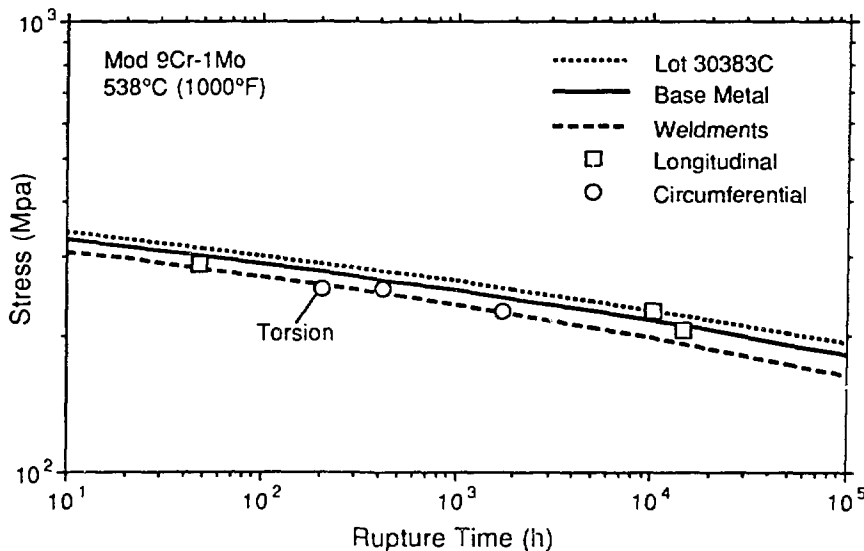
Fig. 3. Equivalent stress vs rupture time for axial or torsional creep-rupture tests of tubular specimens with longitudinal or circumferential welds.

with these values of the creep-strength reduction factor, because they are based on the same model, Eq. (4).

For the four welded-tube tests with $t_r < 2 \times 10^3$ h, the results in Fig. 3 agree very closely with average weldment behavior, thus providing limited confirmation of the adequacy of the creep-strength reduction factors. The two tests with $t_r > 10^4$ h provide additional confirmation and suggest that the factors are somewhat conservative, at least for axial loading of specimens with longitudinal welds, for which strains in weld metal and HAZ are nearly the same.

CONTINUOUS-CYCLING FATIGUE TESTS

To provide additional experimental confirmation of the fatigue-life reduction factor, axial or torsional fatigue tests of 20 tubular specimens with longitudinal or circumferential welds were conducted in air at 538°C (1000°F). Seven tubular specimens without welds were also tested under the same conditions to provide results for direct comparison.

An MTS axial-torsional testing machine was used. The axial fatigue tests were conducted using an MTS high-temperature extensometer for strain control. The torsional fatigue tests were conducted using a capacitive, axial-torsional strain transducer originally developed by K. C. Liu and modified by R. L. Battiste at ORNL. Each device had a gage length of 25.4 mm (1.0 in.). Fully reversed strain cycles were imposed at a Mises equivalent strain rate of 0.001 s^{-1} and four values of Mises equivalent total strain range: 1.5, 1.0, 0.6, and 0.4%.

In Appendix T of Code Case N-47, the Mises definition of equivalent normal strain range is based on the inelastic value of Poisson's ratio, $v = 0.5$. For axial-torsional straining of tubular specimens, this definition reduces to

$$\overline{\Delta \varepsilon} = \sqrt{(\Delta \varepsilon_z)^2 + (\Delta \gamma_{\theta z})^2 / 3} \qquad (5)$$

where $\Delta \varepsilon_z$ is axial strain range and $\Delta \gamma_{\theta z}$ is engineering shear strain range. Since the present tests were either purely axial or purely torsional, the Mises equivalent strain range becomes

$$\overline{\Delta \varepsilon} = \Delta \varepsilon_z, \text{ for } \Delta \gamma_{\theta z} = 0, \qquad (6a)$$

or

$$\overline{\Delta \varepsilon} = \Delta \gamma_{\theta z} / \sqrt{3}, \text{ for } \Delta \varepsilon_z = 0. \qquad (6b)$$

Induction heating was used to maintain a temperature of 538°C (1000°F) at the center of the gage length, and 528°C (982°F) at the ends of the gage length. This difference of 1.2% in absolute temperature was sufficient to ensure that fatigue cracking occurred near the center of the gage length.

To assess the nonuniform strain distribution due to the metallurgical notch, two 25.4-mm (1.00-in.) MTS extensometers were employed in one axial strain-cycling test of a specimen with a circumferential weld. One extensometer was fitted with offset probes to reduce its effective gage length. This device was used to measure average strain in the weld metal, while the other was used to control average strain in the gage length at a range of 0.6%. During the course of the test at 538°C (1000°F), average strain range in the weld metal dropped from about 0.55% to about 0.50%, and hence average strain range in the remainder of the gage length consisting of HAZ rose from about 0.625% to about 0.65%.

Based on visual examination, it was concluded that in each specimen with a circumferential weld or a pair of longitudinal welds, cracking had initiated at a fusion line. In each axial or torsional test of a specimen with a circumferential weld, and in each torsional test of a specimen with longitudinal welds, the crack that led to failure had grown along a fusion line. In each axial test of a specimen with longitudinal welds, the crack had grown in the circumferential direction, crossing a weld. In some of these tests, another crack was observed starting to grow at a fusion line of the other weld, opposite the main crack.

The test results are plotted in Fig. 4(a)-(c) as Mises equivalent total strain range versus cycles to failure, defined as 50% reduction in

maximum axial load or torque. In each figure, different symbols are used to distinguish between tubes with circumferential, longitudinal, or no welds; and, in Fig. 4(c), between axial or torsional loading. Also plotted in each figure are three curves. The uppermost solid line corresponds to the model developed by M.K. Booker at ORNL for uniaxial, continuous cycling of small, solid-bar specimens of modified 9 Cr-1 Mo steel without welds:

$$\Delta \varepsilon_t = A N_f^{-a} + B N_f^{-b} \qquad (7)$$

where $\Delta \varepsilon_t$ is total strain range (%), N_f is cycles to failure, and parameter values are as follows:

A	a	B	b	N_f
0.650	0.0595	52.101	0.598	$\leq 74,652$
0.650	0.0595	0.236	0.117	$> 74,652$

For the tests on which this model is based, complete separation was used as the definition of failure rather than 50% load reduction. The model is considered applicable for fatigue lives of 2×10^2 to 10^8 cycles and temperatures of 22 to 538°C (72 to 1000°F). The intermediate dotted line corresponds to Eq. (8) below, obtained by piecewise reduction of the ORNL model [Eq. (7)] by a factor of two on strain range [Eq. (8c)] or 20 on cycles [Eq. (8a)] and insertion of a smooth transition [Eq. (8b)]. For the present purpose, this curve is unofficially designated the base metal design curve. Officially, the responsibility for establishing such a curve rests with the appropriate ASME Code committees.

$$\Delta \varepsilon_t = A(20N_d)^{-a} + B(20N_d)^{-b}, \text{ for } N_d \leq N_0, \qquad (8a)$$

$$\Delta \varepsilon_t = C N_d^{-c}, \text{ for } N_0 < N_d < 20N_0, \qquad (8b)$$

and

$$\Delta \varepsilon_t = (A N_d^{-a} + B N_d^{-b}) / 2, \text{ for } N_d \geq 20N_0, \qquad (8c)$$

where

$$c = \log 2 / \log 20 = 0.2314 \qquad (8d)$$

$$20N_0 = \left[\frac{(b-c)B}{(c-a)A} \right]^{1/(b-a)} = 14,014 \qquad (8e)$$

$$C = [A(20N_0)^{c-a} + B(20N_0)^{c-b}] / 2 = 2.464 \qquad (8f)$$

and N_d is design allowable cycles. The lowermost dashed line corresponds to Eq. (9) below, obtained by reduction of the base metal design curve [Eq. (8)] by a factor of two on cycles, and is unofficially designated the weldment design curve.

$$\Delta \varepsilon_t = A(40N_d)^{-a} + B(40N_d)^{-b}, \text{ for } 2N_d \leq N_0, \qquad (9a)$$

$$\Delta \varepsilon_t = C(2N_d)^{-c}, \text{ for } N_0 < 2N_d < 20N_0, \qquad (9b)$$

and

$$\Delta \varepsilon_t = [A(2N_d)^{-a} + B(2N_d)^{-b}] / 2, \text{ for } 2N_d \geq 20N_0. \qquad (9c)$$

The values of B and b in Eq. (8c) and (9c) depend on N_d and $2N_d$, respectively, rather than on N_f.

In axial tests [Fig. 4(a)], specimens with circumferential welds had shorter fatigue lives than those with longitudinal welds, which in turn had about the same lives as those with no welds. In torsional tests [Fig. 4(b)], fatigue lives for specimens with circumferential welds were again shortest, but lives for specimens with longitudinal welds were, with one exception, shorter than those with no welds. Each of these patterns seems consistent with the effect of a metallurgical notch. As shown in Fig. 4(c), fatigue lives in axial tests were, with one exception, about the same or less than those in corresponding torsional tests. This is considered typical for
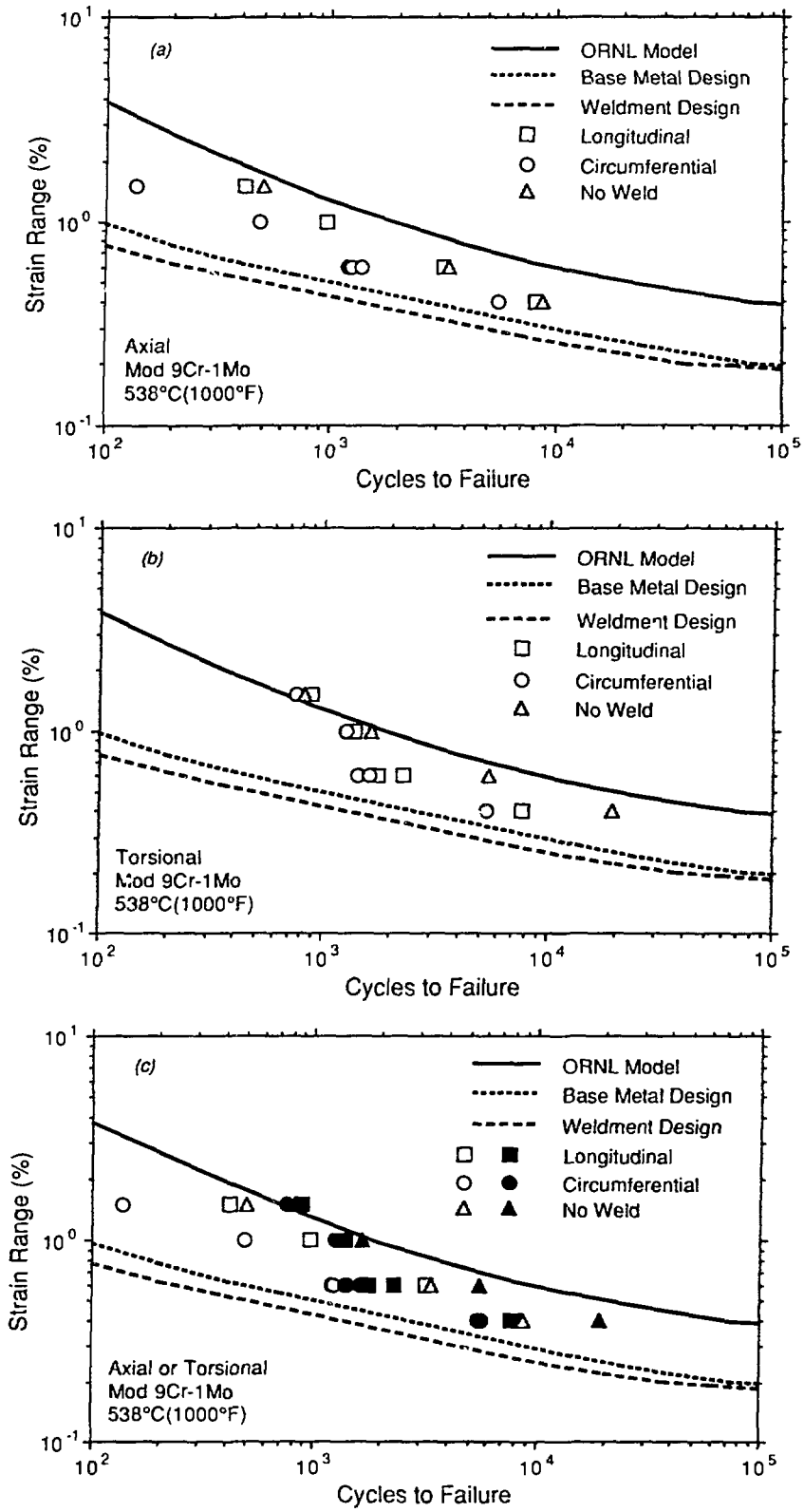
Fig. 4. Mises equivalent strain range vs cycles to failure for fatigue tests of tubular specimens with longitudinal, circumferential, or no welds. (a) Axial tests. (b) Torsional tests. (c) Axial (empty symbols) or torsional (filled symbols) tests.

comparisons based on *Mises* equivalent strain range, and was also observed, for example, with 316 stainless steel (Corum, 1990).

In each of three axial tests [Fig. 4(a)] of tubular specimens without welds, the number of cycles to failure, based on 50% reduction in maximum load, was less than estimated by the ORNL model based on complete separation of small, solid-bar specimens. This difference between observed and estimated fatigue life increases as strain range decreases. Similar results were found for 316 stainless steel (Corum, 1990). The portion of this difference that is due to the definition of failure is thought to be small. The axial test of one tubular specimen without a weld, at a strain range of 0.6%, was continued to complete separation. The number of cycles required to accomplish this was only 5% greater than for 50% reduction in maximum load.

The factor of two on strain range or 20 on cycles used to derive the base metal design curve is intended to cover variables such as surface finish, size, material properties, environment, and fabrication (other than welding). It is obvious from Fig. 4 that the metallurgical notch or other weld effects can consume much of this design margin, and additional margin is needed. The factor of two on cycles used to derive the weldment design curve is intended to provide this margin. In corresponding tests of tubular specimens, the apparent reduction in fatigue life due to weld effects did not exceed a factor of four, and in some cases was less than a factor of two. Similar results were found for 316 stainless steel (Corum, 1990). In all cases there appears to be a reasonable margin between the test results and the weldment design curve.

Like most provisions of Code Case N-47, the weldment fatigue-life reduction factor of two originated in the ASME Code Subgroup on Elevated Temperature Design. It was based primarily on an evaluation of the results of fatigue tests conducted at elevated temperatures on small, solid-bar specimens taken from weldments of austenitic stainless steel (304 and 316) and ferritic steel (2.25 Cr-1 Mo and modified 9 Cr-1 Mo). Although the apparent reduction in fatigue life due to weld effects was greater in some cases, a factor of two was judged to be adequate for structural design, because the specimens and tests were not considered completely representative of welded structures in service (Corum, 1990). The same may obviously be said of the present specimens and tests.

Blass (1990) assessed a definition of equivalent strain range based on the work of Brown and Miller (1973 and 1979). For $\nu = 0.5$, this definition is given by

$$\Delta\varepsilon_{eq} = \left[(2\Delta\gamma'/3)^\beta + (B^\beta - 1)(4\Delta\varepsilon')^\beta\right]^{1/\beta}/B \qquad (10)$$

where $\Delta\gamma'$ and $\Delta\varepsilon'$ are engineering shear and normal components of strain range, respectively, on the planes of maximum shear strain range. By assigning appropriate values to the parameters B and β, this general definition can be made to agree with several specific definitions; and, if suitable test data are available, nonlinear least-squares techniques can be employed to obtain optimum values of B and β for a given material (Blass, 1990).

For axial-torsional straining with $\nu = 0.5$,

$$(2\Delta\gamma'/3)^2 = (2\Delta\gamma_{\theta z}/3)^2 + (\Delta\varepsilon_z)^2 \qquad (11a)$$

and

$$4\Delta\varepsilon' = \Delta\varepsilon_z. \qquad (11b)$$

Substituting Eq. (11) into Eq. (10) with the assigned value $\beta = 2$ results in

$$\Delta\varepsilon_{eq} = \sqrt{(\Delta\varepsilon_z)^2 + (2\Delta\gamma_{\theta z}/3B)^2}. \qquad (12)$$

With $B = 2/\sqrt{3} = 1.155$, Eq. (12) is identical to the corresponding Mises form in Eq. (5). For the present tests

$$\Delta\varepsilon_{eq} = \Delta\varepsilon_z, \text{ for } \Delta\gamma_{\theta z} = 0, \qquad (13a)$$

or

$$\Delta\varepsilon_{eq} = 2\Delta\gamma_{\theta z}/3B, \text{ for } \Delta\varepsilon_z = 0. \qquad (13b)$$

To obtain an optimum value of B based on the results of the present tests of tubular specimens without welds, it is convenient to combine Eq. (13) with

$$\Delta\varepsilon_{eq} = AN_f^{-\alpha}. \qquad (14)$$

Solving for $\log N_f$ gives forms suitable for a linear least-squares fit,

$$\log N_f = [\log A - \log(\Delta\varepsilon_z)]/\alpha, \text{ for } \Delta\gamma_{\theta z} = 0, \qquad (15a)$$

or

$$\log N_f = [\log(3AB/2) - \log(\Delta\gamma_{\theta z})]/\alpha, \text{ for } \Delta\varepsilon_z = 0. \qquad (15b)$$

The results of such a fit are shown in Fig. 5(a). In this figure, $\Delta\varepsilon_{eq}$ given by Eq. (13) with $B = 1.460$ is plotted versus N_f. The empty symbols correspond to axial tests of specimens without welds and the filled symbols to torsional tests. The straight line, corresponding to Eq. (14) with the values $A = 21.81$ and $\alpha = 0.4385$, is not considered applicable much beyond the range of the data in Fig. 5(a). However, the line provides a convenient reference to show that with an optimum value of B, this definition of equivalent strain range can effectively eliminate the disparity between the results of axial and torsional tests typically found with the Mises definition. Moreover, the definition of $\Delta\varepsilon_{eq}$ given by Eq. (10) with $B = 1.460$ and $\beta = 2$, in combination with a more general fatigue-life relation, like Eq. (7), may have much wider applicability.

In Fig. 5(b), the same $\Delta\varepsilon_{eq}$ is used to plot results of the axial or torsional tests of specimens with longitudinal or circumferential welds. In addition to the uppermost solid line that was fitted to the data in Fig. 5(a) for specimens without welds, two other straight lines are plotted. The intermediate dotted line corresponds to reduction of the fitted line by a factor of two on cycles, and the lowermost dashed line by a factor of four. Most of the data in Fig. 5(b) are contained within the band formed by the upper- and lowermost lines and centered on the intermediate line, suggesting again that the weldment fatigue-life reduction factor of two is a reasonable structural design approximation.

CONCLUSIONS

The results of axial or torsional tests of tubular specimens with longitudinal or circumferential welds have provided some needed confirmation of the reduction factors for creep strength and fatigue life of modified 9 Cr-1 Mo steel weldments currently under consideration by appropriate committees of the ASME B&PV Code.

For the modes of loading and weld orientations employed, the creep-strain distributions and rupture-life results seem consistent with the effects of a metallurgical notch. The same is true of cyclic strain range and fatigue life.

The definitions of equivalent normal stress and strain range containing adjustable parameters provided better correlations of the creep-rupture and fatigue lives than the corresponding Mises definitions.
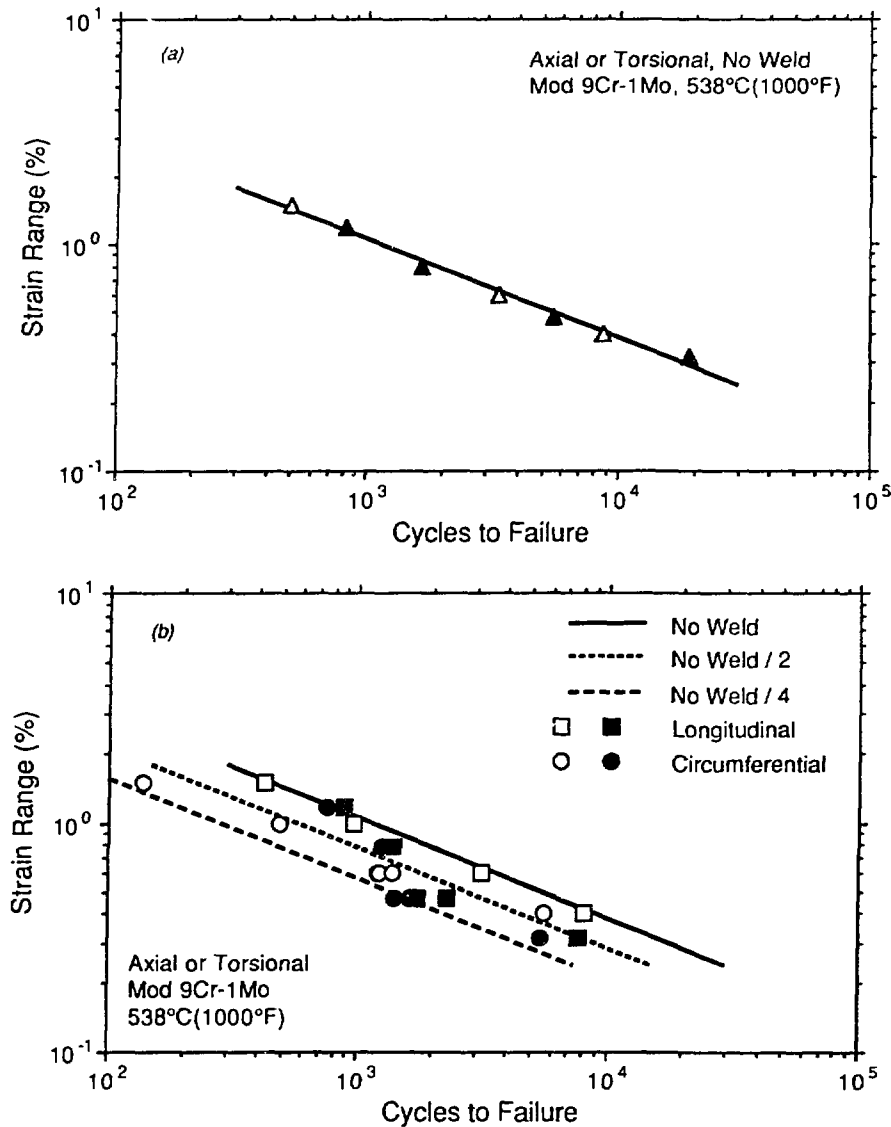
DISCLAIMER

Fig. 5. Equivalent strain range vs cycles to failure for axial (empty symbols) or torsional (filled symbols) fatigue tests of tubular specimens. (a) No welds. (b) Longitudinal or circumferential welds.

REFERENCES

Blass, J. J., 1990, *Multiaxial Fatigue Criterion for 2-1/4 Cr-1 Mo Steel for Use in High-Temperature Structural Design*, ASME Paper 90-JPGC/NE-9.

Brinkman, C. R., Alexander, D. J., and Maziasz, P. J., 1990, *Modified 9 Cr-1 Mo Steel for Advanced Steam Generator Applications*, ASME Paper 90-JPGC/NE-8.

Brown, M.W., and Miller, K. J., 1973, "A Theory for Fatigue Failure under Multiaxial Stress-Strain Conditions," *Proceedings of the Institution of Mechanical Engineers*, Vol. 187 65/73, pp. 745-755; discussion, pp. D229-D244.

Brown, M.W., and Miller, K. J., 1979, "High Temperature Low Cycle Biaxial Fatigue of Two Steels," *Fatigue of Engineering Materials and Structures*, Vol. 1, pp. 217-229.

Corum, J. M., 1990, "Evaluation of Weldment Creep and Fatigue Strength-Reduction Factors for Elevated-Temperature Design," *Journal of Pressure Vessel Technology*, Vol. 112, pp. 333-339.

Huddleston, R. L., 1985, "An Improved Multiaxial Creep-Rupture Strength Criterion," *Journal of Pressure Vessel Technology*, Vol. 107, pp. 421-429.

Huddleston, R. L., 1990, personal communication.

Payne, R. K., 1986, *Low-Cycle Fatigue of Modified 9 Cr-1 Mo Weldments*, Master's Thesis, Georgia Institute of Technology.